Materials
Views
www.MaterialsViews.com

ADVANCED
ENERGY
MATERIALS
www.advenergymat.de

COMMUNICATION

Probing the Mechanism of High Capacitance in 2D Titanium Carbide Using In Situ X-Ray Absorption Spectroscopy

Maria R. Lukatskaya, Seong-Min Bak, Xiqian Yu, Xiao-Qing Yang,* Michel W. Barsoum, and Yury Gogotsi*

The field of supercapacitors (electrochemical capacitors) is constantly evolving. The global motivation is to create devices that possess a significant energy density without compromising the power density.[1] To achieve this goal, new materials must be discovered and complex electrode architectures developed.[2]

Several decades ago, the impressive electrochemical properties of hydrated ruthenium oxide were discovered.[3] Important features of RuO_2 are: (i) good conductivity, which is not typical of transition metal oxides, and (ii) surfaces that participate in reversible redox reactions during charge/discharge, enabling capacitance of 1000 to 1800 F cm^{-3} for thick (>20 μm) electrodes[4] and up to 2800 F cm^{-3} for thin films (50–100 nm).[5] However, the high cost of this material, along with a significant decline in charge storage capacity with increased electrode thicknesses outweighs its outstanding volumetric capacitance, rendering it unsuitable for applications beyond microscale energy storage.[4a]

In search for alternatives, MXenes—a new but quickly expanding family of 2D transition metal carbides (Nb_2C, Ti_3C_2, Ta_4C_3, etc.), captured the attention of researchers recently.[6,7] MXenes possess excellent conductivity and offer a broad variety of chemistries.[7a] MXenes are produced by the selective removal of the atomically thin aluminum layers from the ternary transition metal carbide (MAX phase)[8] structure, e.g., Ti_3AlC_2, via wet chemistry routes, such as etching in HF,[9] NH_4HF_2,[10] or acidic solutions of fluoride salts, i.e., LiF in HCl.[11] The described treatments result in mixed fluorine- and oxygen-containing terminations of transition metal atoms on the MXene surfaces. Thus, the general formula describing MXene composition is $M_{n+1}X_nT_x$, where M is an early transition metal, X is carbon and/or nitrogen, n = 1, 2, or 3, T is surface termination (—F, —OH, =O), and x is number of surface groups per formula unit.[7a]

This combination of terminated transition metal on the surface with a metallically conductive carbide core is believed to be key to the MXenes' promising performance as electrode

materials for energy storage applications, such as Li-ion batteries,[12] Li-S batteries,[13] and supercapacitors.[6] In particular, impressively high volumetric capacitance reaching 900 F cm^{-3} (comparable only with hydrated RuO_2) was measured for $Ti_3C_2T_x$ in aqueous electrolytes.[11,14] Our previous studies revealed that spontaneous intercalation of some cations takes place when MXene samples are exposed to aqueous electrolytes.[6] In situ X-ray diffraction showed that variations of the distance between the $Ti_3C_2T_x$ layers (which is proportional to the c lattice parameter, c-LP) during cycling is small (<5%) and no phase changes were detected.[6] Electrochemical quartz crystal admittance (EQCA) studies of $Ti_3C_2T_x$ multilayer particles in several aqueous electrolytes with different cations revealed that cation insertion is accompanied by electrode deformations (expansion/contraction), facilitated by the presence of water molecules. These deformations occur so quickly, however, that they closely resemble 2D ion adsorption at solid–liquid interfaces.[15] Moreover, it was found that surface chemistry has a significant effect on the capacitive response in acids: decreased amount of F-terminations, relative to those of O and OH, resulted in a significant increase in specific capacitance, i.e., almost doubling it.[14]

These results notwithstanding, the understanding of what fundamental processes are responsible for the promising performance has been lacking. While double layer ion adsorption can be ruled out as the main mechanism, due to the relatively low specific surface area of multistacked MXenes,[6] possible pseudocapacitive storage mechanisms can be hydrogen storage or redox coupled capacitance (**Figure 1**a). In this communication, we report on a set of electrochemical experiments coupled with in situ X-ray absorption spectroscopy (XAS) that shed light on the mechanism of capacitance in $Ti_3C_2T_x$ MXene.
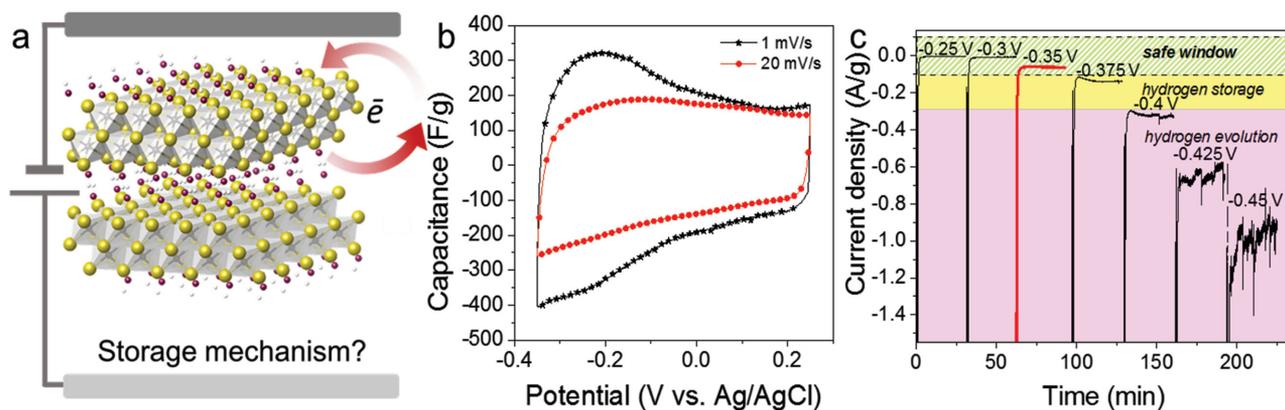
Typical electrochemical performance of the MXenes can be characterized by the nearly rectangular cyclic voltammetry (CV) loops as shown in Figure 1b for $Ti_3C_2T_x$ MXene (produced by etching of Ti_3AlC_2 MAX phase in a LiF-HCl solution)[11] in 1 M H_2SO_4. To ensure that the observed electrochemical behavior is not due to parasitic reactions and also to evaluate possible contributions from hydrogen evolution, a series of constant potential experiments—during which the current change with time was monitored (Figure 1c)—were performed. It is well established that di-hydrogen (H_2) evolution is a faradic process and its intensity (i.e., current) is dependent on the over-potential value. By collecting chronoamperometry (CA) data, at various fixed potentials, a better understanding of the underlying processes can be obtained—as compared to the CV, which unlike CA is dynamic technique: the sample is subjected to a certain potential for no more than several seconds per cycle.

M. R. Lukatskaya, Prof. M. W. Barsoum, Prof. Y. Gogotsi
Department of Materials Science and Engineering
and A. J. Drexel Nanomaterials Institute
Drexel University
Philadelphia, PA 19104, USA
E-mail: gogotsi@drexel.edu
Dr. S.-M. Bak, Dr. X. Yu, Dr. X.-Q. Yang
Chemistry Department
Brookhaven National Laboratory
Upton, NY 11973, USA
E-mail: xyang@bnl.gov

Figure 1. Electrochemical performance of $Ti_3C_2T_x$. a) Schematic of $Ti_3C_2(OH)_2$ structure—where atoms of Ti are yellow, C are gray, and OH are red—and possible contributions of charge transfer to the capacitance, b) cyclic voltammetry of $Ti_3C_2T_x$ in 1 M H_2SO_4 at 1 and 20 mV s^{-1}, and c) chronoamperometry data collected at different potentials.

Based on the observed current density values (Figure 1c), we categorized the potentials at which the CA was performed into three regimes: (i) a "safe" region where the current density does not exceed ≈ 0.1 A g^{-1} (marked in green in Figure 1c) and no H_2 evolution is observed and (ii) a H_2-"storage" region, where the current density is in the 0.1–0.3 A g^{-1} range, (marked in yellow in Figure 1c) and no noticeable bubble formation is observed. In this region, the CA profiles are smooth and can be used when the electrode is cycled at scan rates of $>\approx 20$ mV s^{-1} and (iii) a H_2-evolution region (marked pink in Figure 1c), where the current density >0.3 A g^{-1} and active H_2 evolution is observed. The onset of hydrogen evolution (beginning of Regime 3) limits the cathodic potential for the use of MXene electrode. It is worth noting that this approach of selecting a voltage window and estimating the contributions of various parasitic reactions is applicable to other supercapacitor materials/devices as well. In this case, it allowed us to evaluate the extent of H_2 evolution by simply measuring the current transients, where H_2 bubble formation is mirrored by an uneven current profile. It follows that the lowest negative, and "safe," voltage limit for $Ti_3C_2T_x$ in 1 M H_2SO_4 is −0.35 V versus Ag/AgCl.

As noted above, one of the potential mechanisms for high capacitance is electrochemical hydrogen storage, as has been shown for some carbon materials.[16] However, it is unlikely to have a significant contribution here due to (i) acidity of the electrolyte used: it was reported that hydrogen storage has significant contribution to energy storage only in basic electrolytes and (ii) low specific surface area of MXenes.[16]

We now turn our attention to intercalation pseudocapacitance, i.e., redox processes in the $Ti_3C_2T_x$ during cycling. If that is the case, then Ti atoms would be changing their oxidation state during electrochemical cycling.

In order to investigate this hypothesis, we performed electrochemical in situ X-ray absorption near edge structure spectroscopy (XANES) for the Ti K-edge. XANES is a powerful technique to probe the oxidation states of elements that has been successfully used in the past to shed light on the charge storage mechanism of MnO_2[17] and RuO_2[18] by tracking changes in the metal edge position during electrochemical cycling. Herein, we monitored the shifts in the Ti edge energy at different points of charge and discharge. In situ Ti K-edge XAS spectra were collected—for

a sequence of applied potentials—starting from 0.275 and ending at −0.35 V, and then from −0.2 to 0.345 V on reverse scan, as shown on the CV curve in **Figure 2**a. The Ti K-edge XANES spectra presented in Figure 2b,c feature a relatively weak
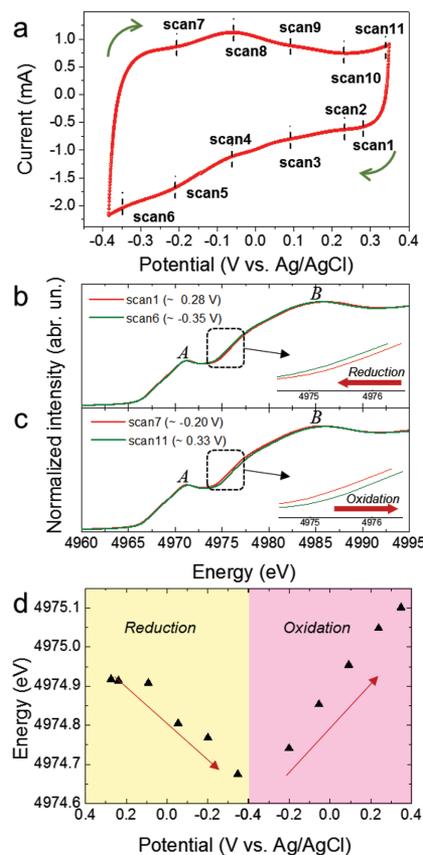
Figure 2. Electrochemical in situ XAS data. a) Cyclic voltammogram collected in in situ XAS electrochemical cell at 1 mV s^{-1} in 1 M H_2SO_4 electrolyte. Ti K-edge XANES spectra were collected, b) between 0.3 and −0.35 V and c) between −0.2 and 0.35 V (vs Ag/AgCl), d) variation of Ti edge energy (at half height of normalized XANES spectra) versus potential during full potential sweep between −0.35 and 0.35 V.

www.MaterialsViews.com

ADVANCED
ENERGY
MATERIALS
www.advenergymat.de

COMMUNICATION
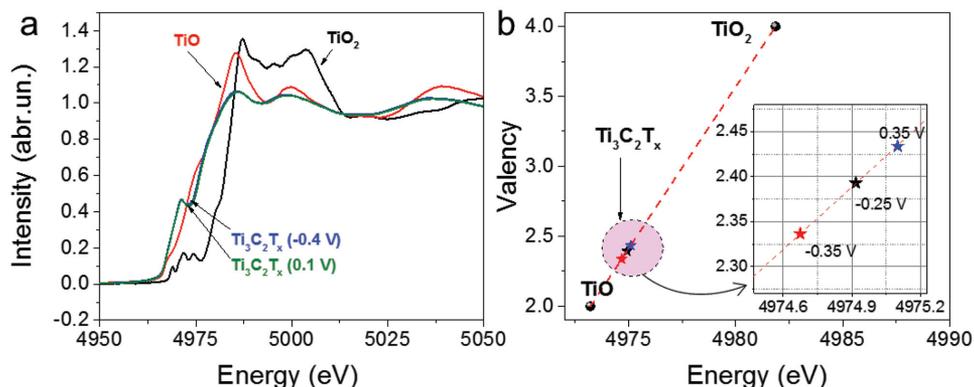
Figure 3. a) Ti K-edge XANES spectra of $Ti_3C_2T_x$ at −0.4 V (blue line) and 0.1 V (green line), together with those of TiO (red line) and TiO_2 (black line). b) Average Ti oxidation state determination in $Ti_3C_2T_x$ at various applied potentials (see inset), using the Ti K-edge energy shift of the reference TiO and TiO_2 compounds.

preedge peak "A" at 4971 eV and a strong main absorption peak "B" at around 4985 eV. The weak preedge absorption involves the hybridization of the metal $3d$ and carbon $2p$ orbitals.[19] Peak "A" can be assigned to the transition of a 1s electron to the hybridized t_{2g} (Ti $3d$ + C $2p$) and e_g (Ti $3d$ + C $2p$) orbitals. The main absorption peak "B," however, is due to the dipole allowed transition of $1s$ electrons to unoccupied Ti $4p$ states.

Although the spectra did not show significant differences in shape, edge shifts were clearly recognized in both charge and discharge potential sweeps (insets in Figure 2b,c). A plot of the Ti K-edge energies, at half height of normalized XANES spectra, versus applied potential (Figure 2d) clearly shows the changes at each potential. Sweeping from 0.275 to −0.35 V, shifts the Ti edge to lower energies. Such a shift is consistent with a decrease in the average oxidation state of the Ti atoms. During the reverse scan to 0.345 V, the XANES spectrum shifts back to the higher energy (and higher Ti oxidation state).

This moderate edge shift in the XANES energy—corresponding to a reduction/oxidation of the Ti—is consistent with our previous study of $Ti_3C_2T_x$ in Li-ion batteries.[20] In that case, an edge shift of ≈0.6 eV was observed over a potential window of ≈3.0 V (vs Li^+/Li) during lithiation (i.e., reduction of Ti).[20]

There is clear change in Ti oxidation state during cycling. To quantify the change, we plotted the Ti K-edge XANES spectra of $Ti_3C_2T_x$ at applied potentials (i.e., −0.4 and 0.1 V) together with the reference Ti oxides (i.e., TiO and anatase TiO_2) in **Figure 3**a. Based on the linear dependence between edge energy and Ti average oxidation state,[21] the latter can be estimated in the MXene sample during cycling (Figure 3b). From the inset shown in Figure 3b, we see that the average oxidation state of Ti changes from 2.33 to 2.43 (i.e., by ≈0.1 $\bar{e}$ per Ti atom) over a 0.7 V window.

To explore the viability of this value we estimate the capacitance using the following formula: $C_g = F\delta/(M_W V)$, where C_g [F g^{-1}] stands for gravimetric capacitance, F [96 485 C mol^{-1}] is Faraday's constant, δ is number of electrons participating in electrochemical reaction (equal to 0.1 × 3 = 0.3 in our case since there are three Ti atoms in $Ti_3C_2T_x$), M_W [g mol^{-1}] is the molar weight, V [V] is voltage window (0.7 V in this case) and the assumed electrochemical reaction is

$$Ti_3C_2O_x(OH)_y F_{2-x-y} + \delta\bar{e} + \delta H^+ \rightarrow Ti_3C_2O_{x-\delta}(OH)_{y+\delta} F_{2-x-y}$$

Since the molar weights for O (16), OH (17), and F (19) are close, the overall formula weight can be assumed to be 202 g mol^{-1}. Thus we get specific capacitance values of 205 F g^{-1}. These values are in a good agreement with the experimental specific capacitances measured herein, which are ≈230 F g^{-1} (when measured in Swagelok cell). Please note that in in situ XAS cell we measured specific capacitance of ≈150 F g^{-1} (for in situ experiments, a hole was drilled in the center of the cell and it was impossible to create a good contact between the electrode and the current collector).

In conclusion, we performed a thorough analysis of the electrochemical behavior of $Ti_3C_2T_x$ and analyzed factors contributing to its capacitance. We demonstrated a procedure for the safe voltage window selection, which can be applied to other electrochemical systems and that provides important insight into electrolyte decomposition processes. Electrochemical in situ XAS measurements detected changes in the Ti oxidation state during cycling. Even though this method is semiempirical and provides a rough estimation, the estimated value is comparable to the value that we calculated from the sample's gravimetric capacitance assuming redox-only capacitance. Therefore, we can conclude that the electrochemical behavior of $Ti_3C_2T_x$ in sulfuric acid is predominantly pseudocapacitive. This renders $Ti_3C_2T_x$ MXene one of very few examples of materials that exhibit "true" pseudocapacitive behavior: it presents a continuous change in the titanium oxidation state during charge/discharge, producing rectangular-shaped CVs. This behavior can be attributed to the 2D nature of $Ti_3C_2T_x$ MXene: spontaneous ion intercalation naturally provides access to electrochemically active transition metal oxide surfaces, while the conductive carbide layer ensures rapid charge transfer. Those properties are not available in titanium oxide or cubic TiC. The results obtained herein are important for another reason: namely, they indicate, as a first approximation, that the average Ti oxidation state in $Ti_3C_2T_x$ is much closer to +2 than +4.

Experimental Section

Electrochemical Measurements: Preliminary electrochemical measurements were performed in a three-electrode Swagelok cell, with

Ag/AgCl as reference electrode, 6 mg $Ti_3C_2T_x$ electrode (containing 5 wt% of polytetrafluoroethylene (PTFE) binder and 5 wt% of carbon black) as working electrode and 33 mg AC (containing 5 wt% of PTFE binder) as counter electrode. During all measurements, the overall cell potential was monitored in order to controllably translate into the two-electrode cell geometry used in the in situ XAS measurements.

In Situ X-ray Absorption Spectroscopy (XAS): In situ Ti K-edge XAS measurement were performed at beamline X18A at the National Synchrotron Light Source (NSLS) of the Brookhaven National Laboratory (BNL) using a Si(111) double-crystal monochromator, detuned to 40% of its original maximum intensity to eliminate high-order harmonics.

The spectroscopic data were collected in fluorescence mode with a passivated implanted planar silicon (PIPS) detector in grazing incident geometry. The PIPS detector was placed normal to the incident beam and at a 45° angle to the sample. The Ti K-edge energy, 4966 eV, was calibrated using the first inflection point of the edge region of a metallic Ti foil recorded before and after measurement.

For the in situ XAS measurements, during electrochemical testing, we used a two-electrode 2032 coin-type cells, with a hole (diameter: 3 mm) drilled on the working electrode side. The MXene served as the working electrode and the activated carbon as the counter electrode. A glass fiber separator (Whatman) was soaked in a 1 M H_2SO_4 aqueous electrolyte. The hole was sealed with a Mylar film.

Detailed information on sample and electrode preparation, electrochemical measurements can be found in the Supporting Information.

Supporting Information

Supporting Information is available from the Wiley Online Library or from the author.

Acknowledgements

[1] P. Simon, Y. Gogotsi, *Nat. Mater.* **2008**, *7*, 845.

[2] J. Yan, Q. Wang, T. Wei, Z. J. Fan, *Adv. Energy Mater.* **2014**, *4*, 43.

[3] S. Hadzi-Jordanov, H. Angerstein-Kozlowska, M. Vukovič, B. E. Conway, *J. Electrochem. Soc.* **1978**, *125*, 1471.

[4] a) J. P. Zheng, P. J. Cygan, T. R. Jow, *J. Electrochem. Soc.* **1995**, *142*, 2699; b) S. H. Oh, L. F. Nazar, *J. Mater. Chem.* **2010**, *20*, 3834.

[5] C. Sassoye, C. Laberty, H. Le Khanh, S. Cassaignon, C. Boissière, M. Antonietti, C. Sanchez, *Adv. Funct. Mater.* **2009**, *19*, 1922.

[6] M. R. Lukatskaya, O. Mashtalir, C. E. Ren, Y. Dall'Agnese, P. Rozier, P. L. Taberna, M. Naguib, P. Simon, M. W. Barsoum, Y. Gogotsi, *Science* **2013**, *341*, 1502.

[7] a) M. Naguib, V. N. Mochalin, M. W. Barsoum, Y. Gogotsi, *Adv. Mater.* **2014**, *26*, 982; b) K. J. Koski, Y. Cui, *ACS Nano* **2013**, *7*, 3739.

[8] M. W. Barsoum, *MAX Phases: Properties of Machinable Ternary Carbides and Nitrides*, John Wiley & Sons, Weinheim, **2013**.

[9] M. Naguib, M. Kurtoglu, V. Presser, J. Lu, J. Niu, M. Heon, L. Hultman, Y. Gogotsi, M. W. Barsoum, *Adv. Mater.* **2011**, *23*, 4248.

[10] J. Halim, M. R. Lukatskaya, K. M. Cook, J. Lu, C. R. Smith, L. A. Naslund, S. J. May, L. Hultman, Y. Gogotsi, P. Eklund, M. W. Barsoum, *Chem. Mater.* **2014**, *26*, 2374.

[11] M. Ghidiu, M. R. Lukatskaya, M. Q. Zhao, Y. Gogotsi, M. W. Barsoum, *Nature* **2014**, *516*, 78.

[12] a) M. Naguib, J. Come, B. Dyatkin, V. Presser, P. L. Taberna, P. Simon, M. W. Barsoum, Y. Gogotsi, *Electrochem. Commun.* **2012**, *16*, 61; b) M. Naguib, J. Halim, J. Lu, K. M. Cook, L. Hultman, Y. Gogotsi, M. W. Barsoum, *J. Am. Chem. Soc.* **2013**, *135*, 15966.

[13] X. Liang, A. Garsuch, L. F. Nazar, *Angew. Chem.* **2015**, *54*, 3907.

[14] Y. Dall'Agnese, M. R. Lukatskaya, K. M. Cook, P. L. Taberna, Y. Gogotsi, P. Simon, *Electrochem. Commun.* **2014**, *48*, 118.

[15] M. D. Levi, M. R. Lukatskaya, S. Sigalov, M. Beidaghi, N. Shpigel, L. Daikhin, D. Aurbach, M. W. Barsoum, Y. Gogotsi, *Adv. Energy Mater.* **2015**, *5*, 1.

[16] K. Jurewicz, E. Frackowiak, F. Béguin, *Appl. Phys. A Mater. Sci. Process.* **2004**, *78*, 981.

[17] a) J.-K. Chang, M.-T. Lee, W.-T. Tsai, *J. Power Sources* **2007**, *166*, 590; b) K.-W. Nam, M. G. Kim, K.-B. Kim, *J. Phys. Chem. C* **2007**, *111*, 749.

[18] Y. Mo, M. R. Antonio, D. A. Scherson, *J. Phys. Chem. B* **2000**, *104*, 9777.

[19] J. G. Chen, *Surf. Sci. Rep.* **1997**, *30*, 1.

[20] Y. Xie, M. Naguib, V. N. Mochalin, M. W. Barsoum, Y. Gogotsi, X. Yu, K. W. Nam, X. Q. Yang, A. I. Kolesnikov, P. R. Kent, *J. Am. Chem. Soc.* **2014**, *136*, 6385.

[21] a) W. J. H. Borghols, D. Lutzenkirchen-Hecht, U. Haake, W. Chan, U. Lafont, E. M. Kelder, E. R. H. van Eck, A. P. M. Kentgens, F. M. Mulder, M. Wagemaker, *J. Electrochem. Soc.* **2010**, *157*, A582; b) W. J. H. Borghols, D. Lutzenkirchen-Hecht, U. Haake, E. R. H. van Eck, F. M. Mulder, M. Wagemaker, *Phys. Chem. Chem. Phys.* **2009**, *11*, 5742.